한국산학기술학회논문지
Vol. 7, No. 1, pp. 7-11, 2006

The SCM Method for Three-Dimensional Dopant Profiles

Jun-Ha Lee[1] and Hoong-Joo Lee[1*]

3차원적 도핑 분포 측정을 위한 SCM 응용 방법

이준하[1], 이흥주[1*]

Abstract Through SCM modeling, we found that the depletion layer in silicon was of a form of a spherical capacitor with the SCM tip biased. Two-dimensional (2D) finite differential method code with a successive over relaxation (SOR) solver has been developed to model the measurements by SCM of a semiconductor wafer that contains an ion-implanted impurity region. Then, we theoretically analyzed the spherical capacitor and determined the total depleted-volume charge Q, capacitance C, and the rate of capacitance change with bias dC/dV. It is very important to observe the depleted carriers' movement in the silicon layer by applying the bias to the tip. So, we calculated the depleted-volume charge, considering different factors such as tip size, oxide thickness, and applied bias (dc+ac), which have an influence on potential and depletion charges.

요 약 SCM(Scanning Capacitance Method)를 이용하여, SCM 팁의 전계에 의해 형성되는 실리콘내의 공핍영역를 분석할 수 있는 방법론을 구축하였다. 2차원 유한요소법을 이용하여 SCM으로 측정된 결과로부터 불순물의 농도를 도출할 수 있었다. 이 방법은 캐패시턴스, 공핍화된 체적 및 바이어스에 따른 캐패시턴스의 변화율로부터 구해진다. 본 연구에서는 팁의 크기, 산화층 두께 및 가해지는 바이어스에 따른 공핍 전하와 전위에 따른 영향등을 분석하였다.

1. INTRODUCTION

As the scaling of feature-size in the gigantic-scale integrated circuits device technology continues, device characterization and life cycle are greatly affected due to an unexpected dopant profile caused by three-dimensional (3D) effects in mask corners and edges. In addition, the need for quantitative 3D impurity dopant profiling is increasing to verify 3D process simulators and to calibrate physical process models used in process simulators. Therefore, an experimentally determined 3D impurity dopant profile needs to estimate these 3D effects precisely. Although several different methods for determining dopant profile, such as tomographic secondary ion mass spectroscopy (SIMS) and nanospreading resistance probe, have been proposed recently, these methods do not yet fully extract quantitative dopant profiles [1,2]. Also, several researchers for two-dimensional (2D) dopant profiling are using a scanning capacitance microscopy (SCM) capacitance-voltage (C-V) measurement method, but these results cannot fully characterize the 2D dopant profiles [3-5]. In addition, because these measurements are performed on the cross-cut sample surface to get 2D dopant profile image, they require a specific sample preparation; that is, these methods are destructive by nature. In this work, we introduce a new dopant profiling method for potentially extracting the 3D dopant profiles. This is a nondestructive method, which is different from the common SCM measurement [6,7].

[1]Department of Computer System Engineering, Sangmyung Univeristy
*Corresponding Author : Hoong-Joo Lee(hjlee@smu.ac.kr)

2. PHYSICAL MODEL FOR 3D

Generally, if one determines the dopant concentration at any position in a depth direction normal to the sample surface, one will know the rate of change of the capacitance with bias changes (dC/dV) at that position by SCM. Therefore, if it is possible to calculate dC/dV through SCM modeling, we can extract 1D dopant profiles, which vary with the depth, by comparing the calculated dC/dV to the measured dC/dV obtained from the SCM output. To do this, it is very important to observe the depleted carriers' movement in the silicon layer by applying a bias to the tip. Therefore, we

calculated the total depleted-volume charges considering different factors, such as tip size, oxide thickness, and applied bias (dc+ac), which have an influence on potential and depletion charge. Now, we present an algorithm to calculate the total depleted-volume charges and dC/dV. First, we assume a 1D Gaussian dopant profile as the initial profile. The Gaussian distribution function is composed of several parameters, such as ion dose (ions/cm^2), peak concentration at the projected ion range, projected ion range (um), and projected standard deviation (um). We determine the depletion-layer width in both the vertical and lateral directions, and calculate the depleted-volume charge Q [8]. The depletion-layer width is defined as the position where the electric field or the band bending potential equals zero. Unlike the case of the parallel plate capacitor, when applying a bias to the very small hemi-spherical SCM tip, the depletion layer in silicon is of the form of a spherical capacitor. Therefore, to calculate the total depleted-volume charges from this capacitor, it is important to define the boundary of the depletion layer in both the vertical and lateral directions. Because the potential distribution in silicon shows 3D symmetry, we developed an algorithm to determine the depleted-volume charge with the biasing voltage using the concentration information given at each position. The procedures are as follows. Applying the bias voltage to the SCM tip, our code solves the 2D nonlinear Poisson's equation and generates the spherical capacitor. We determine the depletion-layer width and its position from the 1D depth profile determined under the tip center and we determine the lateral direction's depletion-layer width based on the previously selected potential position. To interpolate each potential data point, we apply the cubic spline method. After completing the work, we determine the lateral depletion-layer length x from the tip centerline and trace the given potential position in Fig. 1.

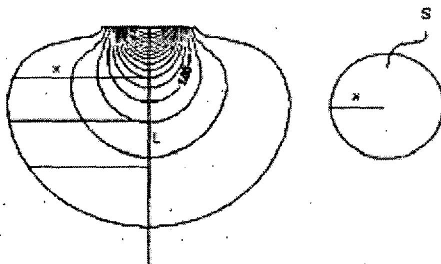

FIG. 1 Depleted carrier volumes were determined from the spherical model, where x is the lateral depletion width from the centerline and L is the disk length.

The length x is a depletion radius at each lateral direction. Once this radius is calculated, we can calculate the total depleted volume that consists of several thin disks, each of which has a small volume element. The i_{th} disk volume Vi and its charge Qi are calculated by multiplying the disk circle area Si by the disk length Li , and by multiplying the disk volume Vi by qn(y), respectively, as follows:

$$\begin{aligned} V_i &= S_i \times L_i, \\ S_i &= \pi x^{2_i}, \\ Q_i &= q n(y) \times V_i, \end{aligned} \tag{1}$$

where q is the elementary charge and n(y) is the dopant concentration at position y from the surface. Therefore, the total depleted-volume charge is

$$Q_i = \sum_{i=1}^{n} Q_i \tag{2}$$

where n is the number of thin disks. Second, we calculate the rate of change of charge with bias voltages. After determining the total depleted-volume charges, we calculate the differential charge changes by applying a differential bias voltage dV to the tip. This is the differential capacitance in a spherical capacitor and is defined as C ≡ dQ/dV. Then, we calculate the rate of change of capacitance with the bias voltage as follows [9]:

$$\begin{aligned} & V \rightarrow Q, \\ V_i = V + \delta V_i &\rightarrow Q_i = Q + \delta Q_i, \\ & C_i \approx \delta Q_i / \delta V_i, \\ V_j = V + \delta V_j &\rightarrow Q_j = Q + \delta Q_j, \\ & C_j \approx \delta Q_j / \delta V_j, \end{aligned} \tag{3}$$

$$\left| \frac{dC}{dV} \right|_{ij} = \frac{C_j - C_i}{\delta V_j - \delta V_i} \tag{4}$$

where Qi and Qj are the total depleted-volume charges at Vi and Vj , respectively, and Ci and Cj are the capacitance in the spherical capacitor. The size of the voltage step dV depends on the applied ac voltage to the SCM tip. Third, we extract a 1D dopant profile comparing the calculated dC/dV to the measured dC/dV according to our inversion model. The procedure of the profile extraction consists of finding the profile that minimizes the least-squares fit criterion like Eq. (5) between the calculated and the measured dC/dV. In other

words, we manipulate the initial Gaussian distribution's parameters until the calculated error is small enough. Finally, we obtain the depth-dependent 1D dopant profile, provided each parameter corresponding to the measured data is determined:

$$\left\| \left(\frac{dC}{dV}\right)_{measured} - \left(\frac{dC}{dV}\right)_{calculated} \right\|^2 < \sum_{V_0}^{V_f} \left(\left\| \left(\frac{dC}{dV}\right)_{measured} - \left(\frac{dC}{dV}\right)_{calculated} \right\|^2 \right) \ll error \qquad (5)$$

If the error is too large for a rapid convergence, we use a previously manipulated Gaussian distribution function or some Pearson distribution function having several parameters. To obtain the lateral (2D) dopant profiles within the measurement zone, we move the SCM tip from row A column 1 (Ra, C1) to row A column 2 (Ra, C2), column 3, etc., as shown in Fig. 2. Then, we extract the 1D dopant profile at these points, based on the method previously used for the 1D dopant profile. After determining the 1D and 2D dopant profiles quantitatively, we extract the 3D dopant profiles by combining these data.

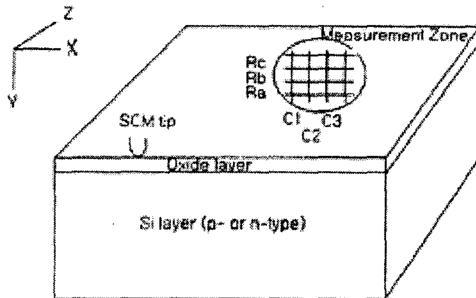

FIG. 2 Block diagram for the 3D dopant profile measurement. Our approach is based on the point-by-point method.

3. RESULTS AND DISCUSSION

Figure 3 shows the contour plot of the electric potential distribution for the various probe-tip sizes. The upper figure shows the potential distribution when the tip size is large (1.4 um). This is based on the parallel-plate capacitor model. The lower figure shows the potential distribution when the tip size is reduced to 100 nm. It indicates that the shape of the potential distribution is changed from the parallel-plate type to the spherical one as the tip size is reduced to a point source. Because the shape of the SCM tip has a 3D geometry, it needs to model the electric potential by using a 3D model. In other words, it requires full 3D modeling, considering not only the depth variation in dopant density, but also the lateral variation to model the tip structure. However, when we assume that all regions' dopant density, except for the mask edges, are nearly uniform in the lateral directions, the shape of the potential distribution generated in a silicon layer has a rotational symmetry around the tip. In this case, the solution can be scaled down to two dimensions. Although this approach is not always applicable, it is useful for reducing the calculation time in solving the nonlinear Poisson's equation. We have calculated the depletion width based on this approach and have observed that when the uniformly doped concentration was 1017 cm23, the generated depletion width was 103 nm (10 nm: 10^{19} cm^{-3}, 2.4 nm: 10^{20} cm^{-3}) at constant 5 V bias. Generally, the higher the dopant density, the shallower the depletion width.

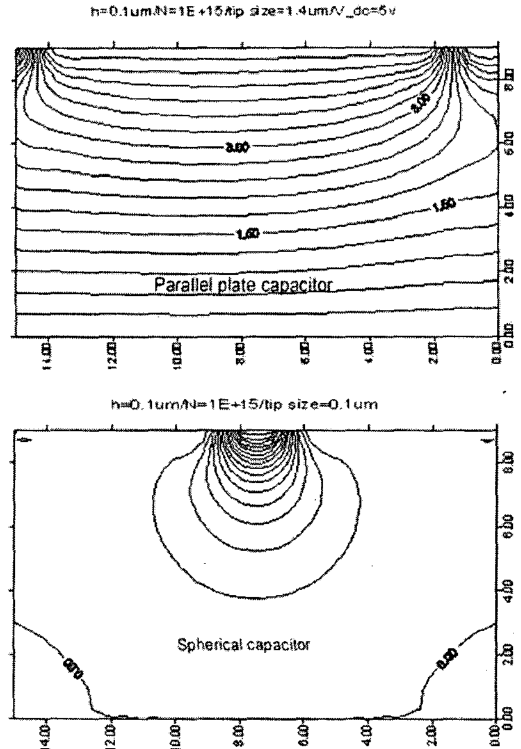

FIG. 3 Comparison of the potential contour plot. The upper part shows a parallel-plate capacitor with a tip size of 1.4 um. The lower part shows a spherical capacitor with a tip size of 100 nm.

Figure 4 shows the depleted volume and the total depleted-volume charges with several uniform impurity concentrations, as calculated by our volume charge determination algorithm. The size of the tip is 10 nm, the thickness of the oxide layer is 11 nm, and the observed bias voltage is 1.5 V.

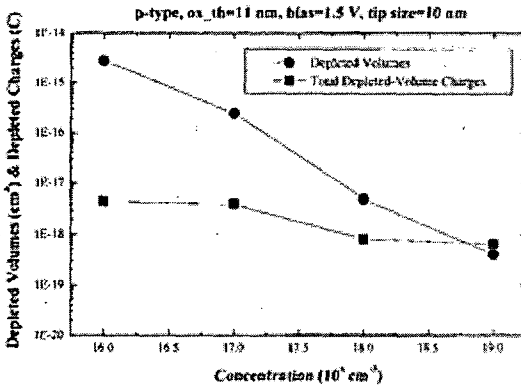

FIG. 4 Total depleted volume and its charges for several impurity concentrations. The filled circles and rectangles show the depleted volumes and the total depleted-volume charges, respectively. These simulation results were obtained at a bias voltage of 1.5 V. The thickness of the oxide layer was 11 nm, and the tip size was 10 nm.

We observed that the lower the dopant density, the larger the depletion layer created by the bias voltage in the spherical capacitor. For higher concentrations (> 10^{18} cm^{-3}), the total depleted-volume charges are concentration independent because the depleted volume is very small, and there are little variations in the total volume charges. It is well known that the spatial resolution of SCM depends on the tip size, and the depleted volume charges would reduce the spatial resolution of SCM at larger bias voltage [3]. Therefore, the SCM measurements for obtaining a surface image are made near the flatband voltages to maintain the spatial resolution. However, our new method for obtaining the quantitative dopant profile is different from that case. Because the smaller the tip size, the less the depleted-volume charges, one must trade off the tip size and the bias voltage properly to implement the new method we proposed. It is important to consider the oxide thickness for the SCM measurement. Figures 5(a) and 5(b) show the total volume charges and capacitance for several oxide thicknesses at uniform dopant density (N=10^{17} cm^{-3}). In the case of a thick oxide layer (> 50 nm), the total volume charges are bias independent and show small variation in capacitance. When the tip size is 10 nm, it is necessary to deposit an oxide layer of less than 25 nm over the silicon surface for SCM.

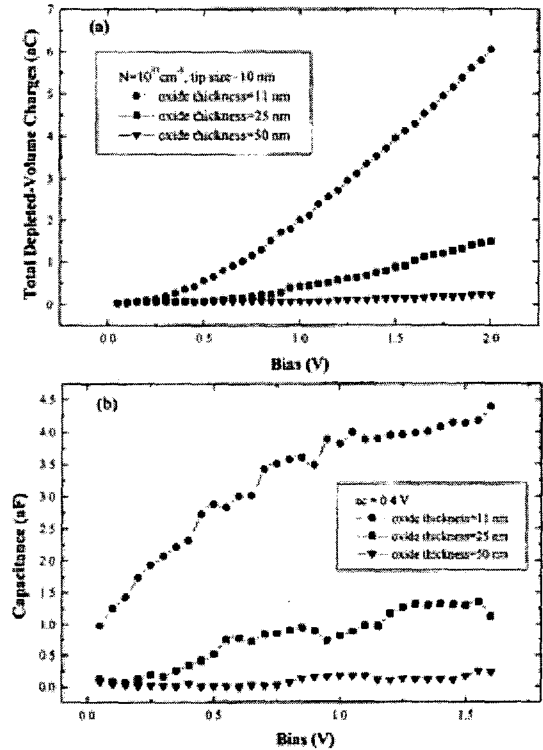

FIG. 5 (a) Calculated total depleted-volume charges for the three different oxide layers of 11, 25, and 50 nm. (b) The calculated capacitance-voltage curves for the three different oxide layers of 11, 25, and 50 nm.

4. CONCLUSION

We have proposed a new technique for extracting 3D dopant profiles based on the common SCM C-V measurement. We have physically analyzed the spherical capacitor and calculated the total depleted-volume charges, capacitance, and rate of change of capacitance with bias voltage in the spherical capacitor model. In addition, we have identified p-type and n-type C-V curves from this model. We found that the C-V curve of the spherical capacitor model is different from that of the parallel-plate capacitor model. The conversion result obtained by using our 1D inversion

algorithm is in good agreement with the SIMS profile, except for the tail region. We completed the basic work for the SCM modeling. Further research on improving of the inversion modeling and verifying the 3D dopant profiles will be done. To do this, we need to analyze the trapped charge in the oxide layer and require a more powerful distribution function, such as the Pearson function, to express the real dopant profile. In addition, we will need to design a full 3D model that considers lateral variation in dopant gradients to compare with the measured SCM data.

REFERENCES

[1] A. C. Diebold, M. Kump, J. J. Kopanski, and D. G. Seiler, Proc.- Electrochem. Soc. **33**, 78 (1994).

[2] R. Subrahmanyan, J. Vac. Sci. Technol. B **10**, 358 (1992).

[3] J. J. Jopanski, J. F. Marchiando, and J. R. Lowney, J. Vac. Sci. Technol. B **14**, 242 (1996).

[4] Y. Huang and C. C. Williams, J. Vac. Sci. Technol. B **12**, 369 (1994).

[5] Y. Huang, C. C. Williams, and J. Slinkman, Appl. Phys. Lett. **66**, 344(1995).

[6] E. H. Nicollian and J. R. Brews, *MOS Physics and Technology* (Wiley, New York, 1982).

[7] J. F. Marchiando, J. Res. Natl. Inst. Stand. Technol. **100**, 661 (1995).

[8] I. D. Mayergoyz, J. Appl. Phys. **59**, 195 (1986).

[9] N. Khalil, J. Faricelli, and C. L. Huang, J. Vac. Sci. Technol. B **14**, 224 (1996).

Jun-Ha Lee [Regular member]

He received his B.S, M.S and Ph.D degrees in Electronic Engineering from Chung-Ang University. His research interests include semiconductor processes, and device and circuit technology. He is currently an assistant professor at Sangmyung University.

Hoong-Joo Lee [Life member]

He received his B.S and M.S degrees from Hanyang University and his Ph.D degree in electrical engineering from State University of New York at Buffalo, respectively. His research interests include semiconductor materials and solar energy generation. He is currently an associate professor at Sangmyung University.